

# Temperature-based Instanton Analysis: Identifying Vulnerability in Transmission Networks

Jonas Kersulis,  
Ian Hiskens

Elec. Eng. and Computer Science  
University of Michigan  
Ann Arbor, MI, United States

Michael Chertkov,  
Scott Backhaus

Center for Nonlinear Studies  
Los Alamos National Laboratory  
Los Alamos, NM, United States

Daniel Bienstock

Ind. Eng. and Operations Research  
Columbia University  
New York, NY, United States

**Abstract**—A time-coupled instanton method for characterizing transmission network vulnerability to wind generation fluctuation is presented. To extend prior instanton work to multiple-time-step analysis, line constraints are specified in terms of temperature rather than current. An optimization formulation is developed to express the minimum wind forecast deviation such that at least one line is driven to its thermal limit. Results are shown for an IEEE RTS-96 system with several wind-farms.

**Index Terms**—Forecast uncertainty, Optimization, Transmission operations, Wind energy

## I. INTRODUCTION

The prevalence of renewables in modern transmission networks has researchers and system operators asking: What happens when the wind changes, and could fluctuations harm the grid? The instanton problem provides an answer, and this paper extends instanton analysis to the temporal setting. Though small deviations from wind forecasts are typically harmless, it is possible for certain wind generation patterns to drive the system to an insecure operating point. Out of all troublesome wind generation patterns, the one that deviates least from the forecast is called the instanton. Instanton analysis uses optimization to find the set of troublesome wind patterns, each of which causes a particular line to encounter its flow limit. By ranking these wind patterns according to distance from forecast, we can characterize the system's vulnerability to forecast inaccuracy and enhance system operator awareness.

The instanton problem was initially considered in [1] and [2] where a DC power flow approximation was used to turn instanton analysis into a convex problem with an analytic solution. The physically accurate AC power flow formulation was used in [3], with an iterative scheme required for finding instanton candidates. Current instanton research is exploring the trade-off between problem complexity and solution accuracy, with the goal of developing the most accurate model that remains convex (and therefore guarantees a solution). Instanton work to date has focused on instantaneous vulnerability by seeking to find the smallest wind generation change that drives a line to its power or current limit. Thus, the troublesome wind patterns uncovered by such instanton analysis may be fleeting.

It is safe to temporarily operate a line above its current limit. Transmission system operators know this and periodically allow lines to operate above their limits to promote smooth operation under heavy, though temporary, flow patterns (see the introduction of [4] for a history of dynamic line rating starting in the 1970s). It takes time for line conductors to heat sufficiently that they sag to an unacceptable level (as defined by statute and nearby tree limbs). As long as the line is allowed to cool before reaching this point, no harm will be done. If an operator is comfortable with temporarily overloaded lines, information from existing instanton analysis may be too conservative to aid decision making.

In this paper we bring instanton analysis into the temporal setting. We consider multiple time steps and replace line current limits with heat constraints. A line's temperature is a function of heat input (primarily Ohmic losses and heat from the sun) and dissipation (convection and radiation, which depend on ambient conditions), and is represented as a differential equation (see Section 3.4 of [5] for a standard set of equations governing line temperature dynamics). Ohmic loss heating is related to power flow analysis via angle difference variables. By modeling line temperature over an appropriate time horizon, the proposed method discovers multiple-time-step wind patterns that are both likely to occur and sure to induce excessive sag for at least one line in the network.

The remainder of the paper describes the temporal instanton problem (Section II), translates it into an optimization problem (Section III), presents a solution method (Section IV), and illustrates temporal instanton analysis using a modified RTS-96 network (Section V).

## II. PROBLEM FORMULATION

Section II-A describes an approximate line loss formulation that forms the basis of a dynamical model developed in Section II-B. Finally, Section II-C incorporates line temperature dynamics into a complete mathematical model.

### A. Line losses

Starting with the AC line loss expression, [6] derived the following approximate relationship between line losses and

---

The authors acknowledge the support of the Los Alamos National Laboratory Grid Science Program, subcontract 270958.

TABLE I  
LINE HEATING PARAMETERS

Parameter	Units	Description
$T_s$	$s$	Sample time
$mC_p$	$J/(m \cdot C)$	Per-unit-length heat capacity of the conductor
$\eta_c$	$W/(m \cdot C)$	Conductive heat loss rate coefficient
$\eta_r$	$W/(m \cdot C)$	Radiative heat loss rate coefficient
$T^{\text{lim}}$	$C$	Line temperature at steady-state current limit.
$\Delta q_{s,ij}$	$W/m$	Solar heat input into conductor
$\Delta T_{\text{amb}}$	$C$	Change in ambient temperature

voltage angle differences for line  $(i, j)$ :

$$f_{ij}^{\text{loss}} \approx r_{ij} \left( \frac{\theta_{ij}}{x_{ij}} \right)^2. \quad (1)$$

In this expression,  $f_{ij}^{\text{loss}}$  is the approximate active power loss on the line;  $\theta_{ij}$  is the difference between angles  $\theta_i$  and  $\theta_j$ ; and  $r_{ij} + jx_{ij}$  is the impedance of the line between nodes  $i$  and  $j$ . Three assumptions underpin (1): voltage magnitudes are all 1 pu, cosine may be approximated by its second-order Taylor expansion, and  $x_{ij} \geq 4r_{ij}$ . Thus, (1) uses DC power flow assumptions to approximate line losses, but remains nonlinear.

### B. Line temperature dynamics

According to analysis in [6] (which is based on [5]), changes in line temperature may be approximated using Euler integration:

$$\Delta T_{ij}[t+1] = \tau_{ij} \Delta T_{ij}[t] + \rho_{ij} \Delta f_{ij}^{\text{loss}}[t] + \delta_{ij} \Delta d_{ij}[t], \quad (2)$$

where the initial condition is  $\Delta T_{ij}[0] = 0$ . Constants  $\tau_{ij}$  and  $\bar{\gamma}_c$  are defined as,

$$\tau_{ij} = 1 - \frac{T_s \bar{\gamma}_c}{mC_p}, \quad \bar{\gamma}_c = \eta_c + 4\eta_r (T^{\text{lim}} + 273)^3, \quad (3)$$

where  $\rho_{ij} = T_s/mC_p$ . Finally,  $\Delta d_{ij} = [\Delta q_{s,ij} \quad \Delta T_{\text{amb}}]^\top$ , and  $\delta_{ij}$  represents exogenous inputs and is equal to  $[\rho_{ij} \quad \gamma_{ij}]$ , where

$$\gamma_{ij} = \frac{T_s \bar{\gamma}_a}{mC_p}, \quad \bar{\gamma}_a = \eta_c + 4\eta_r (T_{\text{amb}}^* + 273)^3. \quad (4)$$

Integration sample time is constrained by numerical stability requirements, which necessitate  $\tau_{ij} \in (-1, 1)$ :

$$T_s < \min_{ij} \left\{ \frac{2mC_{p,ij}}{\bar{\gamma}_{c,ij}} \right\}. \quad (5)$$

Table I summarizes the line temperature parameters in (2)-(5).

Assuming line parameters and ambient conditions are independent of the power flow, (2) is driven by network conditions through the angle difference variables  $\theta_{ij}[t]$ . Repeated substitution and use of (1) yields an expression for the change in line temperature at a final time in terms of angle differences

at all other time steps. If there are  $T$  total time steps, this relationship may be expressed as:

$$\Delta T_{ij}[T] = \frac{\rho_{ij} r_{ij}}{x_{ij}^2} \sum_{t=1}^T \tau_{ij}^{t-1} \theta_{ij}^2[T+1-t] + \delta_{ij} \sum_{t=1}^T \tau_{ij}^{t-1} \Delta d_{ij}[T+1-t]. \quad (6)$$

The first term in (6) varies with angle differences. The second term, which is based on external conditions, is constant with respect to power flow. Switching the order of summation and moving constants to the left side yields

$$\Delta T_{ij}[T] - \delta_{ij} \sum_{t=1}^T \tau_{ij}^{T-t} \Delta d_{ij}[t] = \frac{\rho_{ij} r_{ij}}{x_{ij}^2} \sum_{t=1}^T \tau_{ij}^{T-t} \theta_{ij}^2[t]. \quad (7)$$

This summation may be written in matrix form by defining an angle difference vector, a constant vector, and a coefficient matrix:

$$\boldsymbol{\theta}_{ij} := [\theta_{ij}[1] \quad \theta_{ij}[2] \quad \cdots \quad \theta_{ij}[T]]^\top \quad (8a)$$

$$\boldsymbol{\Delta} d_{ij} := [\Delta d_{ij}[1] \quad \Delta d_{ij}[2] \quad \cdots \quad \Delta d_{ij}[T]]^\top \quad (8b)$$

$$\boldsymbol{\tau}_{ij} := \text{diag}([\tau_{ij}^{T-1} \quad \tau_{ij}^{T-2} \quad \cdots \quad 1]). \quad (8c)$$

In terms of these newly-defined symbols (whose dependence on  $T$  is hidden for conciseness), (7) becomes,

$$\Delta T_{ij}[T] - \delta_{ij} \boldsymbol{\Delta} d_{ij}^\top \boldsymbol{\tau}_{ij} \mathbf{1} = \frac{\rho_{ij} r_{ij}}{x_{ij}^2} \boldsymbol{\theta}_{ij}^\top \boldsymbol{\tau}_{ij} \boldsymbol{\theta}_{ij}. \quad (9)$$

The left side of (9) is constant with respect to power flow, while the right side is a weighted, scaled two-norm of the vector of angle difference variables  $\boldsymbol{\theta}_{ij}$ .

The approximate line temperature dynamics developed here will be used in Section III to model line temperature over an optimization horizon.

### C. Instanton formulation

The preceding discussion developed an approximate line loss expression to relate line temperature to angle variables according to (9). Here we describe the remaining parts of the temporal instanton model.

The following equations describe an optimization problem that minimizes deviation from the wind forecast while heating a certain line to a specified (limiting) temperature:

$$\min_{\text{dev}} \sum_{t=1}^T \text{dev}_t^\top Q_{\text{dev}} \text{dev}_t \quad (10a)$$

subject to:

$$\sum_j Y_{ij} \theta_{ij,t} = G_{i,t} + R_{i,t} + \text{dev}_{i,t} - D_{i,t} \quad (10b)$$

$$\forall i \in 1 \dots N, t \in 1 \dots T$$

$$G_t = G_{0,t} + k\alpha_t \quad \forall t \in 1 \dots T \quad (10c)$$

$$\theta_{ref,t} = 0 \quad \forall t \in 1 \dots T \quad (10d)$$

$$\Delta T_{ij}[T] = \Delta T_{ij}^{\text{lim}} \quad \text{for some } (i, j) \in \mathcal{G} \quad (10e)$$

where:

- $dev_{i,t}$  is the difference between actual output and forecast output at wind-farm  $i$  and time  $t$ . Thus,  $dev_t$  is the vector of wind forecast deviations at time  $t$ .
- $Q_{dev}$  may be set to the identity matrix or used to encode correlation between wind sites.
- $R_{i,t}$  is renewable generation forecast at bus  $i$  and time  $t$ .
- $Y_{ij}$  is the  $(i,j)$ -th element of the admittance matrix, which assumes zero resistance.
- $\theta_{ij,t}$  is the difference between voltage angles  $\theta_i$  and  $\theta_j$  at time  $t$ .
- $G_{i,t}$  is conventional active power generation at node  $i$  and time  $t$ , and  $G_t$  is a vector including all nodes.
- $D_{i,t}$  is active power demand at bus  $i$  and time  $t$ .
- $N$  is the number of buses (nodes).
- $G_{0,t}$  is scheduled conventional active power generation (without droop response).
- $k$  is the vector of participation factors for conventional generators, with  $\sum_i k_i = 1$ . (The case where  $k_i = 1$  corresponds to generator  $i$  taking all slack.)
- $\alpha_t$  is the power mismatch at time  $t$ .
- $\Delta T_{ij}^{lim}$  is the change in temperature that will push line  $(i,j)$  to its thermal limit.
- $\theta_{ref}$  is the voltage angle of the reference bus.
- $\mathcal{G}$  is the set of edges (lines).

Equation (10a) expresses the desire to find wind patterns that remain close to the wind forecast. The first constraint equation (10b) enforces DC power balance. The next constraint (10c) models conventional active power generation as a sum of scheduled generation and droop response (where generators share the task of compensating for mismatch between total generation and load). The system angle reference is established by (10d). Last is (10e), which constrains the temperature of a particular line to be equal to its limit at the final time  $T$ . Using (9) we can express (10e) as

$$\Delta T_{ij}^{lim} - \delta_{ij} \Delta d_{ij}^T \tau_{ij} \mathbf{1} = \frac{\rho_{ij} r_{ij}}{x_{ij}^2} \theta_{ij}^T \tau_{ij} \theta_{ij}. \quad (11)$$

Thus, (10) has a quadratic objective function, a set of linear constraints, and a single quadratic constraint. By solving (10) for each line in the network, we obtain a set of instanton candidate wind patterns, each of which will heat a particular line to its thermal limit. Of these candidates, the one that deviates least from the wind forecast (across all time steps) is the instanton wind pattern.

The form of (10) suggests a QCQP optimization formulation. The next section establishes this QCQP.

### III. CONVERSION TO OPTIMIZATION PROBLEM

Previous instanton work relied on convex optimization to quickly find instanton wind patterns. Heat-constrained temporal instanton analysis is more complicated: it cannot be formulated as anything simpler than a quadratically-constrained quadratic program (QCQP). QCQPs are NP-hard in general; reasonable solutions may exist, but unless the quadratic constraint matrices are positive-definite there is no solution guar-

antee (see [7]). Because system operators require robustness, “no solution found” is an unacceptable output. With this criterion in mind, we proceed to develop an optimization model whose structure permits us to find solutions despite nonconvexity.

With all deviation, angle, and mismatch variables stacked into a single vector, (10) takes the form:

$$\min z^T Q_{obj} z \quad (12a)$$

$$s.t. \quad Az = b \quad (12b)$$

$$z^T Q_{\theta} z = c. \quad (12c)$$

The objective (12a) is equivalent to (10a), the linear equality constraints (12b) represent (10b)-(10d), and the quadratic equality constraint (12c) is equivalent to (10e). The vector  $z$  consists of  $(N + N_R + 2)T$  variables, where  $N$  is the number of nodes,  $N_R$  is the number of nodes with wind-farms, and  $T$  is the number of time steps. Note that  $N_R T$  of the variables represent deviations from forecast at each wind-farm and time step. There are also  $NT$  angle variables (of which  $T$  are fixed to zero according to (10d)) and  $T$  mismatch variables  $\alpha_t$  (one per time step). The last  $T$  variables are auxiliary angle difference variables used to convert (10e) into a norm constraint; they are defined later in (15).

Variables may be stacked in any order. One convenient ordering is  $T$  groups of  $(N + N_R + 1)$  variables, with the  $T$  auxiliary angle difference variables at the end. At a particular time step  $t$ , the group of  $(N + N_R + 1)$  variables is  $[dev_t^T \ \theta_t^T \ \alpha_t]^T$ , with  $dev_t$  representing deviations from forecast at the  $N_R$  wind nodes,  $\theta_t$  is the column of  $N$  angle variables at time  $t$ , and  $\alpha_t$  is the mismatch between generation and demand at time  $t$ .

The remainder of this section describes the components of (12). The objective matrix  $Q_{obj}$  is described in Section III-A, linear constraint parameters  $A$  and  $b$  are considered in Section III-B, and the constraint matrix  $Q_{\theta}$  is addressed in Section III-C.

#### A. Objective function and $Q_{obj}$

The objective function depends solely on deviation variables, so  $Q_{obj}$  is a matrix that weights only the  $dev$  variables in  $z$ . If there are two time steps, for example, the vector of variables would be  $z = [dev_1^T \ \theta_1^T \ \alpha_1 \ dev_2^T \ \theta_2^T \ \alpha_2 \ \hat{\theta}]^T$ , and  $Q_{obj}$  would be,

$$Q_{obj} = \begin{bmatrix} Q_{dev} & 0 & 0 & 0 & 0 & 0 \\ 0 & 0 & 0 & 0 & 0 & 0 \\ 0 & 0 & 0 & 0 & 0 & 0 \\ 0 & 0 & 0 & Q_{dev} & 0 & 0 \\ 0 & 0 & 0 & 0 & 0 & 0 \\ 0 & 0 & 0 & 0 & 0 & 0 \end{bmatrix}.$$

Note that  $Q_{dev}$  represents the correlation between wind-farms (if any). In the Section IV numerical analysis, we will assume  $Q_{dev} = I$ , the identity matrix.

## B. Linear constraints: $A$ and $b$

All constraints except the temperature limit may be grouped into a single linear system  $Az = b$ . Setting aside the  $T$  auxiliary variables for the moment, the  $A$  matrix has a block diagonal structure where each block consists of  $(N + 1)$  rows and  $(N_R + N)$  columns. The first  $N$  rows describe power balance and distributed slack behavior at each node. For node  $i$  and time  $t$ , we fix elements of  $A$  and  $b$  to establish

$$\sum_j Y_{ij} \theta_{j,t} = (G_{i,t}^0 + k_i \alpha_t) + (R_{i,t} + dev_{i,t}) - D_{i,t}. \quad (13)$$

The first pair of terms on the right-hand side of (13) represents conventional generation with distributed slack (generator  $i$  is taking a portion  $k_i$  of the mismatch  $\alpha_t$ ). The second pair of terms is renewable generation: forecast  $R_{i,t}$  plus deviation  $dev_{i,t}$ . The final term is demand at node  $i$  and time  $t$ . (Note that renewable generation terms are zero for nodes without wind-farms.) In addition to the  $N$  rows corresponding to (13) at the  $N$  nodes, there is one additional equation associated with time  $t$  that fixes the angle reference:

$$\theta_{ref,t} = 0. \quad (14)$$

The  $(N + 1)$  rows of  $Az = b$  expressed in (13) and (14) pertain to a single time step  $t$ , with  $T$  blocks of this form arranged diagonally to form  $(N + 1)T$  rows of  $A$  and the corresponding  $b$  vector. There is one additional block of  $A$  used to define auxiliary angle difference variables  $\hat{\theta}_{ij,t}$  in terms of angle variables  $\theta_{i,t}$  and  $\theta_{j,t}$  at each time step:

$$\hat{\theta}_{ij,t} = \tau^{\frac{T-t}{2}} (\theta_{i,t} - \theta_{j,t}). \quad (15)$$

The next subsection explains why these variables are helpful.

## C. Quadratic constraint: $Q_\theta$ and $c$

Recall that (11) describes the temperature constraint on a chosen line  $(i, j)$ . We can rearrange (11) into the form of (12c), with all constants on the right side:

$$\theta_{ij}^\top \tau_{ij} \theta_{ij} = \frac{x_{ij}^2}{\rho_{ij} r_{ij}} \left( \Delta T_{ij}^{\text{lim}} - \delta_{ij} \Delta \mathbf{d}_{ij}^\top \tau_{ij} \mathbf{1} \right) \quad (16)$$

This makes it clear that the appropriate value of  $c$  in (12c) is

$$c = \frac{x_{ij}^2}{\rho_{ij} r_{ij}} \left( \Delta T_{ij}^{\text{lim}} - \delta_{ij} \Delta \mathbf{d}_{ij}^\top \tau_{ij} \mathbf{1} \right) \quad (17)$$

From the definition of  $\hat{\theta}_{ij,t}$  in (15), we see that the left side of (16) may be expressed as  $\hat{\theta}_{ij}^\top \hat{\theta}_{ij}$ . Thus, if the  $\hat{\theta}_{ij}$  variables are placed at the bottom of  $z$ ,  $Q_\theta$  must be a matrix of zeros with a  $T$ -by- $T$  identity matrix in the lower-right corner. This ensures that  $z^\top Q_\theta z = \hat{\theta}_{ij}^\top \hat{\theta}_{ij}$ , as desired.

Section II described the temporal instanton problem, Section III expressed it as a QCQP, and this section defined each component. Next we present a solution method for (12).

## IV. SOLUTION

The structure of (12) is similar to that of the well-known trust region subproblem. Here we describe a four-step solution method based in part on [8]. We begin by considering the vector of variables  $z$  as three groups:  $z_1 \in \mathbb{R}^{N_R T}$  contains all wind deviations,  $z_2 \in \mathbb{R}^{(N+1)T}$  contains angle and mismatch variables, and  $z_3 \in \mathbb{R}^T$  contains auxiliary angle difference variables involved in line temperature calculation. (This partition of  $z$  is independent of how the variables are ordered.) With this notation, the problem becomes

$$\min z_1^\top Q_z z_1 \quad (18a)$$

$$s.t. \quad Az = b \quad (18b)$$

$$z_3^\top z_3 = c, \quad (18c)$$

where  $Q_z$  is  $Q_{dev}$  repeated in block-diagonal fashion  $T$  times.

Several changes of variables may be used to obtain an equivalent form of (18) whose solution is straightforward.

### A. Translation

The first step is to change variables from  $z$  to  $y = z - z^*$ , where  $z^* \in \{z : Az = b\}$ . This translation transforms  $Az = b$  into  $Ay = 0$ . To prevent the change from introducing a linear term into the quadratic constraint, we require  $z_3^* = 0$ . To satisfy  $Az^* = b$ , the subvectors  $z_1^*$  and  $z_2^*$  must satisfy,

$$A \begin{bmatrix} z_1^* \\ z_2^* \\ 0 \end{bmatrix} = b.$$

It is straightforward to find a min-norm  $z^*$  that satisfies this constraint by partitioning and factorizing  $A$  appropriately. After translation, the problem becomes

$$\min y_1^\top Q_z y_1 + 2y_1^\top Q_z z_1^* \quad (19a)$$

$$s.t. \quad Ay = 0 \quad (19b)$$

$$y_3^\top y_3 = c. \quad (19c)$$

### B. Kernel mapping

The form of (19b) suggests an intuitive explanation: any solution to (19) must lie in the nullspace (kernel) of  $A$ . If  $\dim \mathcal{N}(A) = k$  is the dimension of this nullspace, we can let  $y = Nx$  where the  $k$  columns of  $N$  span  $\mathcal{N}(A)$ . (Note that  $x$  does not refer to reactance in this context.) This change of variables is akin to a rotation, but reduces the problem dimension to  $k$ . Partitioning  $N$  according to,

$$\begin{bmatrix} y_1 \\ y_2 \\ y_3 \end{bmatrix} = \begin{bmatrix} N_1 \\ N_2 \\ N_3 \end{bmatrix} x$$

allows (19) to be written,

$$\min x^\top (N_1^\top Q_z N_1) x + 2x^\top (N_1^\top Q_z z_1^*) \quad (20a)$$

$$s.t. \quad x^\top N_3^\top N_3 x = c. \quad (20b)$$

All feasible solutions to (20) lie in the nullspace of  $A$ , so the linear constraints are now implicit.

### C. Obtaining a norm constraint

After kernel mapping, the quadratic constraint is no longer a norm constraint. This can be corrected in two steps. First, perform an eigendecomposition  $N_3^\top N_3 = UDU^\top$  and let  $\hat{x} = U^\top x$ . The constraint is diagonal in terms of  $\hat{x}$ :

$$x^\top N_3^\top N_3 x = \hat{x}^\top D \hat{x} \quad (21)$$

where  $D$  is diagonal and has at most  $T$  nonzero elements, so the right side of (21) may be expanded into:

$$\begin{bmatrix} \hat{x}_1^\top & \hat{x}_2^\top \end{bmatrix} \begin{bmatrix} 0 & 0 \\ 0 & \hat{D} \end{bmatrix} \begin{bmatrix} \hat{x}_1 \\ \hat{x}_2 \end{bmatrix}. \quad (22)$$

The second step is to change variables from  $\hat{x}$  to  $w = [w_1^\top w_2^\top]^\top$ . The variables  $x$ ,  $\hat{x}$  and  $w$  are related through:

$$\begin{bmatrix} w_1 \\ w_2 \end{bmatrix} = \begin{bmatrix} I & 0 \\ 0 & \hat{D}^{1/2} \end{bmatrix} \begin{bmatrix} \hat{x}_1 \\ \hat{x}_2 \end{bmatrix} = K \hat{x} \quad (23)$$

$$\implies w = KU^\top x.$$

(Note that  $x = UK^{-1}w$  because  $UU^\top = I$ .) In terms of  $w$ , (20b) is transformed through (21) to give the form of a norm:

$$\hat{x}^\top D \hat{x} = \hat{x}_2^\top \hat{D}^{1/2} \hat{D}^{1/2} \hat{x}_2 = w_2^\top w_2. \quad (24)$$

Of course, this change of variables must also be applied to the cost function. After substitution and simplification, the full problem becomes:

$$\min w^\top B w + w^\top b \quad (25a)$$

$$s.t. w_2^\top w_2 = c \quad (25b)$$

where

$$B = K^{-1}U^\top N_1^\top Q_z N_1 U K^{-1} \text{ and } b = 2K^{-1}U^\top N_1^\top Q_z z_1^*.$$

The manipulations in this section have restored the norm structure of the quadratic constraint. In the next section we use the KKT conditions of (25) to eliminate  $w_1$ , the unconstrained part of  $w$ . This will allow us to write the objective in terms of  $w_2$  only.

### D. Eliminating $w_1$

Note that  $w_1$  is unconstrained in (25). For a fixed  $w_2$ , we can use the KKT conditions to find  $w_1$  such that the objective is minimized. Begin by expanding the objective:

$$\begin{aligned} f(w) &= [w_1^\top \ w_2^\top] \begin{bmatrix} B_{11} & B_{12} \\ B_{12}^\top & B_{22} \end{bmatrix} \begin{bmatrix} w_1 \\ w_2 \end{bmatrix} + [w_1^\top \ w_2^\top] \begin{bmatrix} b_1 \\ b_2 \end{bmatrix} \\ &= w_1^\top B_{11} w_1 + 2w_1^\top B_{12} w_2 + w_2^\top B_{22} w_2 \\ &\quad + w_1^\top b_1 + w_2^\top b_2. \end{aligned}$$

Next, set the partial derivative with respect to  $w_1$  equal to zero:

$$\begin{aligned} \frac{\partial f}{\partial w_1} &= 2w_1^\top B_{11} + 2w_2^\top B_{12}^\top + b_1^\top = 0 \\ \implies w_1 &= -B_{11}^{-1} \left( B_{12} w_2 + \frac{1}{2} b_1 \right). \quad (26) \end{aligned}$$

After substitution of (26), the objective depends only on  $w_2$ :

$$\begin{aligned} f(w_2) &= w_2^\top (B_{22} - B_{12}^\top B_{11}^{-1} B_{12}) w_2 \\ &\quad + w_2^\top (b_2 - B_{12}^\top B_{11}^{-1} b_1). \end{aligned}$$

(Note that the constant term, which plays no role in minimization, was omitted.) The full optimization problem becomes:

$$\min w_2^\top \hat{B} w_2 + w_2^\top \hat{b} \quad (27a)$$

$$s.t. w_2^\top w_2 = c, \quad (27b)$$

where

$$\hat{B} = B_{22} - B_{12}^\top B_{11}^{-1} B_{12} \text{ and } \hat{b} = b_2 - B_{12}^\top B_{11}^{-1} b_1.$$

This is a QCQP in  $T$  dimensions with a single norm constraint. It is straightforward to obtain solutions to this problem, as the next subsection shows.

### E. Solution via enumeration

A straightforward method of solving (27) involves initially diagonalizing  $\hat{B}$  through an eigendecomposition. It will be assumed that step has been completed.

Let  $v$  be the Lagrange multiplier associated with (27b) and write the first-order optimality condition for (27):

$$\begin{aligned} \frac{\partial \mathcal{L}(w_2, v)}{\partial w_2} &= 2\hat{B} w_2 + \hat{b} - v(2w_2) = 0 \\ \implies \hat{B} w_2 + \frac{1}{2} \hat{b} &= v w_2. \quad (28) \end{aligned}$$

Equation (28) is a linear system that yields  $w_2$  for fixed  $v$ :

$$w_{2,i} = \frac{\hat{b}_i/2}{v - \hat{B}_{i,i}}. \quad (29)$$

In addition to satisfying (29), an optimal  $w_2$  must satisfy the quadratic constraint. Substituting (29) into (27b) yields the ‘‘secular equation’’ (see [8]):

$$s(v) = \sum_i \left( \frac{\hat{b}_i/2}{v - \hat{B}_{i,i}} \right)^2 = c. \quad (30)$$

Note that  $s(v)$  has one pole per unique nonzero diagonal element of  $\hat{B}$ . There are at most two solutions per pole, one on each side. This is best understood graphically. Figure 1 illustrates a three-pole secular equation taken from analysis of the RTS-96 network. The Lagrange multiplier  $v$  is on the horizontal axis, and the secular equation value  $s(v)$  is on the vertical. Solutions are intersections of  $s(v)$  with the horizontal line  $s(v) = c$ . They can be computed numerically with a simple binary search algorithm.

## V. RESULTS FOR RTS-96 NETWORK

We used data from [9] to demonstrate temporal instanton analysis on a wind-augmented RTS-96 network model. Consider a scenario unfolding over three time steps: first the wind forecast is 50% of some nominal value, next it is equal to the nominal value, and finally it is scaled to 150% of nominal. Throughout this wind ramping, generator dispatch and demand remain constant. Temporal instanton analysis with

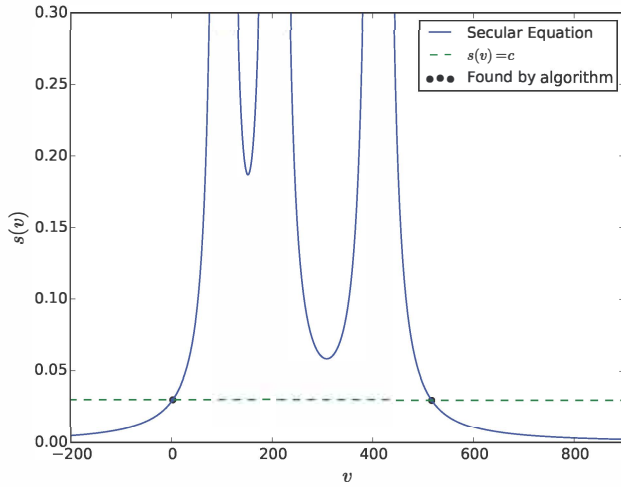


Fig. 1. Plot of secular equation for a single line in the RTS-96. Note that  $s(v)$  approaches infinity at the three poles, and there could be as many as six solutions if  $c$  were large enough.

$c = 0.03$  and  $\tau = 0.5$  indicates that the line between buses 121 and 325 is most susceptible to excessive heating under these conditions. In other words, of all dangerous wind patterns that could occur during the wind ramp, the most likely is a pattern that overheats the line between buses 121 and 325. Figure 1 illustrates the secular equation used to find this instanton pattern, and Figure 2 shows the system state at the second time step. The largest deviation in the instanton pattern is 0.73 pu, well within the range of wind forecast values (whose maximum is 1.2 pu).

## VI. CONCLUSIONS

The paper has extended instanton analysis to consider the temperature dynamics of overloaded lines. The resulting formulation is a quadratically constrained quadratic program (QCQP). A computationally cheap algorithm has been developed for obtaining candidate solutions of this QCQP. There is a great deal of flexibility in the temporal instanton model that has yet to be explored. In future work we plan to include transformers, consider the effects of ambient conditions in greater detail, and test the limits of the algorithm using larger networks with many time steps.

## REFERENCES

- [1] M. Chertkov, F. Pan, and M. Stepanov, "Predicting failures in power grids: The case of static overloads," *IEEE Transactions on Smart Grid*, vol. 2, no. 1, pp. 162–172, Mar. 2011.
- [2] M. Chertkov, M. Stepanov, F. Pan, and R. Baldick, "Exact and efficient algorithm to discover extreme stochastic events in wind generation over transmission power grids," in *Proc. 2011 50th IEEE Conference on Decision and Control and European Control Conference (CDC-ECC)*, 2011, pp. 2174–2180.
- [3] S. Baghsorkhi and I. Hiskens, "Analysis tools for assessing the impact of wind power on weak grids," in *Proc. Systems Conference (SysCon)*, 2012 *IEEE International*, 2012, pp. 1–8.
- [4] H. Banakar, N. Alguacil, and F. Galiana, "Electrothermal coordination part I: theory and implementation schemes," *IEEE Transactions on Power Systems*, vol. 20, no. 2, pp. 798–805, May 2005.

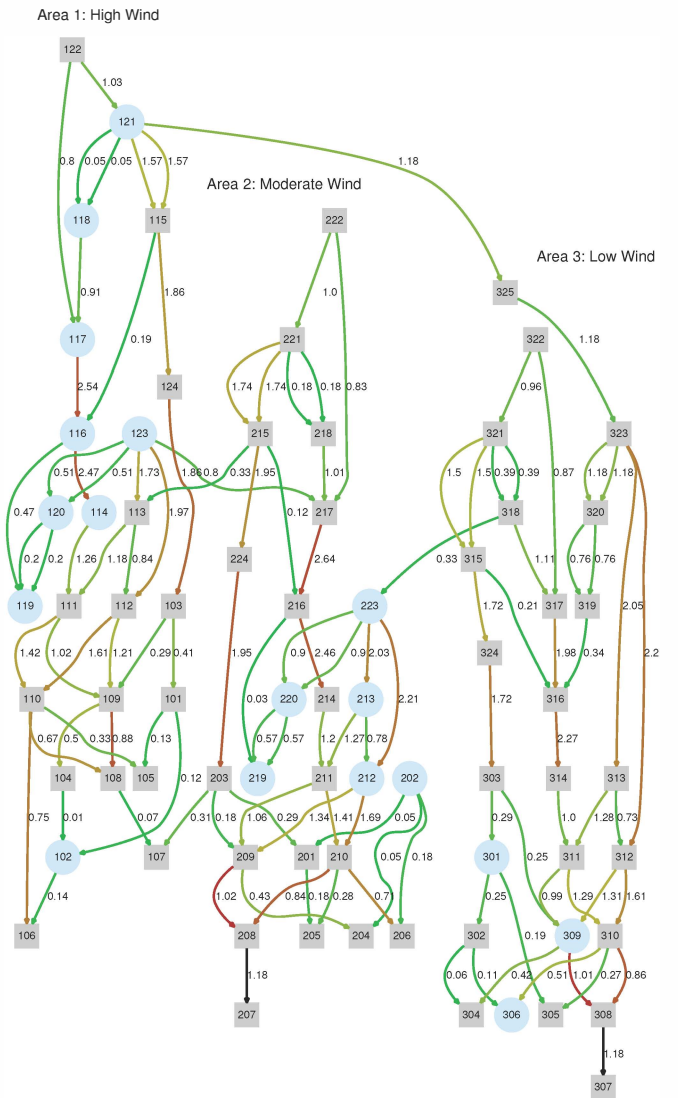


Fig. 2. Graph depiction of RTS-96 system state under instanton conditions at time step 2 of 3. The stressed line is between buses 121 and 325 (top center). wind-farms are indicated by blue, and lines are colored according to how close their flows are to static active power limits.

- [5] "IEEE standard for calculating the current-temperature of bare overhead conductors," *IEEE Std 738-2006 (Revision of IEEE Std 738-1993)*, pp. c1–59, Jan. 2007.
- [6] M. Almassalkhi and I. Hiskens, "Model-predictive cascade mitigation in electric power systems with storage and renewables – part I: Theory and implementation," *IEEE Transactions on Power Systems*, vol. PP, no. 99, pp. 1–11, 2014.
- [7] O. Mehanna, K. Huang, B. Gopalakrishnan, A. Konar, and N. Sidiropoulos, "Feasible point pursuit and successive approximation of non-convex QCQPs," *IEEE Signal Processing Letters*, vol. PP, no. 99, pp. 1–1, 2014.
- [8] D. Bienstock and A. Michalka, "Polynomial Solvability of Variants of the Trust-region Subproblem," in *Proceedings of the Twenty-Fifth Annual ACM-SIAM Symposium on Discrete Algorithms*, ser. SODA '14. Portland, Oregon: SIAM, 2014, pp. 380–390. [Online]. Available: <http://dl.acm.org/citation.cfm?id=2634074.2634102>
- [9] H. Pandzic, Y. Dvorkin, T. Qiu, Y. Wang, and D. Kirschen, "Unit Commitment under Uncertainty - GAMS Models, Library of the Renewable Energy Analysis Lab (REAL), University of Washington, Seattle, USA. [Online]. Available: [http://www.ee.washington.edu/research/real/gams\\_code.html](http://www.ee.washington.edu/research/real/gams_code.html)